Research on Engineering Structures & Materials
www.jresm.org
Research Group

Technical Note

Optimal positioning and distribution of magnetorheological damper

Chandan K[1,a], Daniel C*[1,2,b], Anuroop P[2,c], S. Vivekananda Sharma[1,3,d], Arunraj E[1,e], Hemalatha G[1,f]

[1]*Department of Civil Engineering, Karunya Institute of Technology and Sciences, Coimbatore, India*
[2]*Department of Civil Engineering, Hindustan Institute of Technology and Science, Chennai, India*
[3]*Department of Civil Engineering, National Institute of Technology Meghalaya, Shillong, India*

Article Info

Article history:

Received 30 Jan 2024
Accepted 10 July 2024

Keywords:

Magnetorheological (MR) damper;
MR damper placement;
Semi-Active control;
Equation of motion

Abstract

During seismic events, devices are used to disperse energy in buildings, reducing structural damage and preventing collapse. One such device is the magnetically polarizable particle damper, consisting of a hydraulic cylinder filled with magnetically responsive particles in fluid. Recent research optimized damper placement and distribution using detailed mathematical modeling and mode shapes covering over 95% of the building's mass. Researchers identified critical damper positions by correlating these models with maximum force functions in the equations of motion. The study proposed a positioning strategy to reduce costs associated with damper installation in typical building practices. The number of dampers required varied with applied loads: 20kN, 30kN, 90kN, and up to 200kN. For instance, under 20kN and 30kN loads, optimal distribution included assigning 8 dampers to the ground, first, second floors, decreasing to 4 on floors three and four, and 2 on the fifth floor, totaling 14 and 20 dampers, respectively. Optimization values for these loads were calculated at 17.71. Dealing with a 90kN load required 44 dampers, distributed as 8 on lower levels, 4 on the third floor, and 8 each on floors four and five. Remarkably, while 20kN and 30kN damper counts reduced, 24 were added for 90kN, yielding an optimization score of 45.84. For a 200kN load, 17 dampers were strategically allocated, with specific placements adjusted per floor, achieving an efficiency score of 49.616. This underscores the effectiveness of the chosen damper arrangement in bolstering structural resilience against seismic forces.

1. Introduction

Studies pertaining to earthquakes are essential for comprehending seismic hazards, which aids in determining the possible threats to life and property. This research covers a wide range of topics, including ground motion prediction, fault line detection, and seismicity patterns. They offer insightful information on the probability and severity of earthquakes in particular areas [1]. Building designs that can survive seismic pressures and resilient infrastructure are made possible by research in earthquake engineering. This covers developments in material science, structural engineering, and retrofitting methods meant to reduce mortality and damage during seismic occurrences. Significant material losses, such as collapsing structures, occur in areas vulnerable to strong earthquakes, a problem that contemporary engineering finds difficult to address. [2-4]. This is a more comprehensive illustration of how magneto-rheological dampers are used in civil engineering to reduce the seismic response of buildings during earthquakes. As

*Corresponding author: danielckarunya@gmail.com
[a] orcid.org/0009-0001-1496-0681; [b] orcid.org/0000-0002-4024-4742; [c] orcid.org/ 0009-0002-0986-4537;
[d] orcid.org/0000-0003-4923-621X; [e] orcid.org/0000-0001-7067-3786; [f] orcid.org/0000-0001-7067-3786
DOI: http://dx.doi.org/10.17515/resm2024.168ma0130tn

electromagnetically controlled shock absorbers, MR dampers enhance safety by reducing unanticipated displacements to guarantee livable circumstances. [5-8]. The development of control devices with practical applications has been the focus of major efforts throughout the past few decades. For their capacity to absorb energy and lessen structural reactions in buildings and bridges, passive devices such as base isolation, metallic yield dampers, friction dampers, visco-elastic dampers, viscous dampers, tuned mass dampers, and tuned liquid dampers have been the subject of much research. Although these devices produced good results, they showed limits when it came to changing patterns and loads. [8-12]. Variable orifice dampers, variable stiffness devices, and electro-rheological and magneto-rheological fluid dampers are examples of semi-active devices that provide more adaptability and dependability than their passive equivalents. Magneto-Rheological (MR) fluid damper as shown in Fig. 1. One proposed semi-active control device that shows promise is the magnetorheological damper. It is controlled by a magnetic field, usually produced by an electromagnet, and includes magnetorheological fluid [13–17]. With this configuration, the power of the electromagnet may be continuously adjusted to change the damping properties of the shock absorber. However, due to financial limitations, it is not feasible to place MR dampers at every joint due to their high cost, which is impacted by different fluid characteristics. Therefore, in order to achieve cost-effective distribution, it is imperative to optimize their placement throughout multiple levels. [18-20].

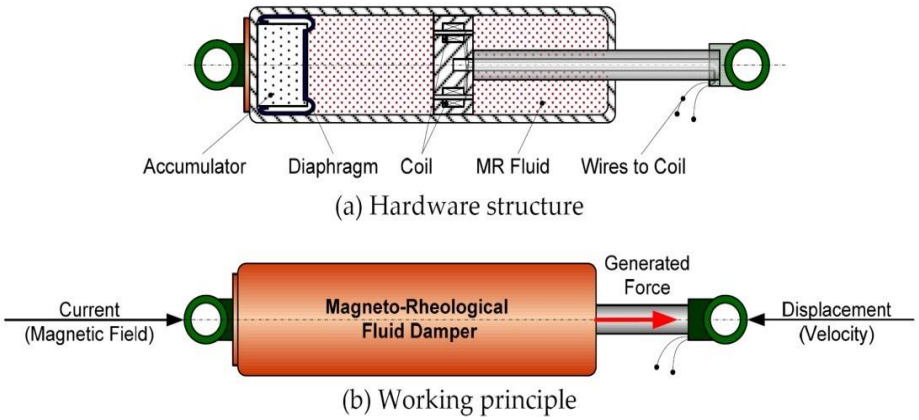

Fig. 1. Magneto rheological damper and its principle [21]

In this work, the forces acting on the joints of the structure are analyzed, and a methodical approach to positioning the MR damper for maximum damper efficiency is proposed. A magnetorheological (MR) damper's hardware normally consists of components as shown in Fig 1: The MR damper's internal components are contained and shielded by the outside shell. To endure mechanical loads, it is usually composed of steel or other robust materials. Within a cylinder that contains MR fluid is a piston assembly that moves. The piston aids in regulating the MR fluid flow via the damper. One part that keeps MR fluid in reserve under pressure is the accumulator. In the accumulator, the diaphragm divides the gas or air from the MR fluid. It guarantees that the MR fluid stays under pressure and keeps gas or air from combining with the fluid. The cylinder is surrounded by an electromagnetic coil. The coil creates a magnetic field that changes the viscosity of the MR fluid when an electric current is supplied to it. A suspension of magnetic particles with a size of microns suspended in a carrier fluid, such silicone or oil, is known as an MR fluid. The MR fluid's viscosity varies in response to a magnetic field, enabling modification of its damping properties. The electromagnetic coil is connected to a power supply and control device via electrical connections. These cables provide the coil with the electricity it needs to create

the magnetic field that regulates the MR fluid's damping characteristics. The study consists of the process that entails calculating the general equation of motion to fully represent each floor's natural displacement, and then utilizing matrix methods to validate the findings to assure correctness. The analytical approach incorporates many methodologies, such as benchmarking to IS1893:2002 criteria for base shear and load distribution, determining the point of contra flexure, and considering external force function impacts based on seismic loading. The modal mass distribution of MR dampers is established by extensive mathematical modeling and modal mass computations. This modal mass ensures effective damper use throughout the structure by acting as a criterion for load breakdown and damper distribution. Motivated by energy conservation concepts like the transmission of energy between colliding metallic balls, an algorithm is designed to strategically install dampers, mainly along extreme columns. To further inform the distribution strategy, participation variables are considered to evaluate the role that mass plays in the structure's responsiveness to external influences. Project advances show optimization under various conditions; higher efficiency is shown in situations with several damper versions. Thorough mapping and data processing offer a thorough picture of damper distribution on every floor, guaranteeing implementation feasibility and economy.

2. Methodology

The goal of this research is to fully represent the general equation of motion mathematically in order to comprehend the natural displacement of each floor. This entails employing matrix techniques to validate the correctness of the displacement, velocity, and acceleration solutions. Correlating mode shapes and examining force functions at maximum boundary circumstances are used to reduce the number of dampers. The emphasis is on utilizing MATLAB calculations, which are provided in an MS-Excel sheet, to identify crucial places for the placement of dampers and to build an optimal distribution plan across floors. The goal of MS-Excel's data analysis and charting is to make fieldwork more efficient. A benchmark building is used in the research for these inquiries is shown in Fig. 2.

3. Methods for Analysis

The displacement or frequency of seismic loads on the structure affects how far the point of contra flexure is from the highest floor. Only when ground acceleration is greater than natural frequency does structural deformation occur; the external forces that have the greatest effect are sinusoidal and are referred to as the force function [22]. The main positioning restriction is determined by using IS1893:2002 [25] to determine base shear and load distribution. This entails determining how shear is distributed throughout floors. Positioning recommendations are verified at several joints and locations with varying lateral seismic stresses. The mode forms covering more than 95% of mass are identified and examined for association with the equation of motion's maximum boundary conditions. This determines the best location for dampers across floors.

The analyzed data is shown to show the relationship between the modal mass of each floor and the capabilities of different dampers. An Excel document has a detailed record of the joint placement. The maximum modal mass and base shear are given priority in this technique, which serves as a constraint for the placement and distribution of dampers. Since a structure might have an endless number of mode forms, it is not realistic to study them all; thus, it is important to choose one by thorough mathematical modeling that encompasses over 95% of the mass. This entails using an exponential function as the force function and a sine to solve the general equation of motion.

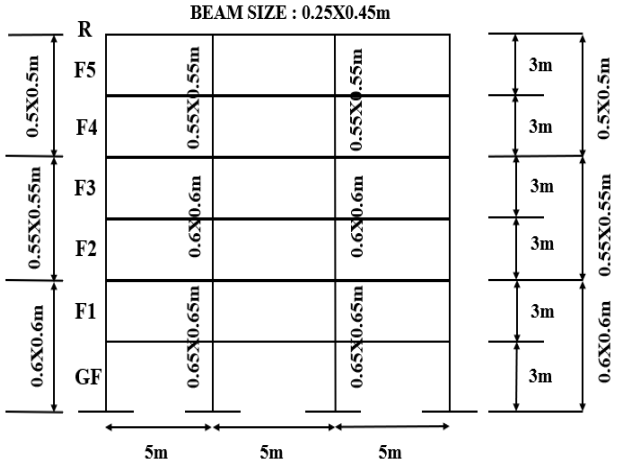

Fig. 2. Benchmark G+5 building

The specific integral and complementary function are two components of the mathematical method that equally contribute to the result. In order to properly address non-trivialities, a quadratic characteristic equation of degree 2 and order 1 is used in this specific integral.

- Case1: Applying excessive sufficiency to a linear equation of degree 1 and order 1 causes mathematical uncertainty, as the solution might not satisfy all equations on separate levels.
- Case 2: If a third-degree polynomial were taken into account, the equation would need to be solved with at least three floor loads. This would limit the equation's application to six-story buildings and render it inappropriate for structures with fewer floors, which is outside the purview of our study.

Therefore, based on the justification provided, it was determined that the second degree equation, which has degree 1 and order 1, is more appropriate for the current situation and is used to solve the current problem. The left-hand linear differential equation can be used to obtain the expression's complementary function.

$$(m * D^2 + c * D + k) * x = 0 \tag{1}$$

must be resolved by taking into account each disparity with regard to ‘x’ as ‘D’ where ‘m' represents the mass, 'c' represents the damping coefficient, 'k' represents the stiffness, 'D' represents the differential operator, and 'x' represents the displacement and solving it for its solution i.e.

$$\frac{-b \pm \sqrt{b^2 - (4 * a * c)}}{2 * a} \tag{2}$$

after which the obtained values of D can be retraced by integrating and solve the obtained solution for 2 different constants (since the degree of the differential equation is 2).

3.1 Mode Shape

The mode shape which contains more than 95% involvement of the mass of the given structure then that mode can be used for analysis and can proceed for further mathematical modelling, and the mode is generally assumed as most probable mode. since

for a given structure there will be infinite number of modes due to non-triviality of the particular integral of the solution since all the mode shapes cannot be analyzed for it is identified as the cumbersome job, so in order to analyze all the mode shapes of the structure a mode that contains more than ninety-five percent of the mass involvement is found out and taken for obtaining the same for further proceedings

3.2 Equation of Motion

The terms involved are mass(m), damping(c), stiffness(k), displacement or lateral deflection(x), velocity ($\dot{x}$), acceleration ($\ddot{x}$), force function (f(t)), here the force function is taken as the combination of sine function followed by exponential function. Reason for sine function is among all the earthquake data available the trigonometric function involving sine or cosine was found to give the worst results for its wave form of intensified load pattern, so it's chosen for this case [23].

$$m\ddot{x} + c\dot{x} + kx = f(t) \tag{3}$$

This is general equation of motion that is used here for all the six slabs of the structure, in fact this is not an equation it's an expression because the right-hand side had the force function involved. It was generally termed to be equation since mostly in all the calculations involved only the complementary function part of the solution was considered as the complete solution. There is the case where the complete solution i.e. complementary solution as well as force function is also used as its significance is elucidated in the following subheadings.

3.3 Complementary Function

This is one part of the solution which generally contributes 50% of the solution to the given problem depending on the degree of uncertainty involved in the problem. If no ambiguity was identified for available unknowns and chosen knowns of the problem, then complementary function of the solution is assumed to be the complete solution i.e. if no trace of non-triviality. Since our case of problem involves almost a due uncertainty it is mandatory to consider the integral to sum up to the existing complementary function. Roots:

$$r_{1,2} = \frac{-c}{m} \pm \sqrt{\frac{c^2}{4m^2} - \frac{k}{m}} \tag{4}$$

General solution:

$$x = p * e^{r_1 t} + q * e^{r_2 t} \tag{5}$$

Modified solution

$$x=A*\sin(\omega t) + B*\cos(\omega t) \tag{6}$$

Since imaginary function involved in the above roots. Final complementary function (C.F):

$$x=A*\sin(\omega t) + B*\cos(\omega t) \tag{7}$$

complementary function gives the information on the roots obtained for given equation of motion considering only the left-hand side equating to zero to assume it for quadratic nature of the equation. since the roots are equated to the differential function (D) of the existing equation it has to be solved to obtain the 'x' value for different time periods, after which the constant must be solved for extreme boundary conditions (time taken for highest amplitude (1st amplitude generally taken) of the structure). since

$$e^{ix} = p * cos(\omega t) + i * sin(\omega t) \tag{8}$$

in the root's 'r' will be imaginary, if the equation was evaluated for zero damping, temporarily it was considered as zero (after which analyzed for 5% of damping force i.e. 0.05) in this case to avoid the uncertainty for obtaining the solution, after putting the E7 in the E5 the solution was modifies as shown in the E6. since the modified solution i.e. E6 contains a greater number of unknowns than the available knowns it triggers the uncertainty of the problem to solve.

3.4 Particular Integral

This part of the solution contributes to almost fifty percent of the complete solution which contains the solvation of the force function for differential terms in the denominator. The differential terms include the skeletal part of the left-hand side of the expression i.e. only the differential inclusion of the LHS is taken to the denominator of the integral. Since both the terms of consideration in the force function are empirical in nature i.e. ambiguous in nature it needs the solvation by differential chain rule by justifiable choosing of the first and second term. After evaluation as per the above procedure the final integral was identified as,

$$\frac{e^{-t}sin(\omega t)}{mD^2 + k} \tag{9}$$

In the above-mentioned expression D is not a variable but it is a differential form with respect to 'x', which again must be solved for different variables for different floors which has been tabulated in

3.5 Characteristic Equation

Characteristic equation is generally adopted when there is ambiguity in solvation of the linear differential equation depending on the number of unknowns and available or chosen knowns.

The choice of this characteristic equation comes to play when the uncertainty in the solvation arises, here in this case in the part of solution i.e. complementary function the equation E6 is identified as ambiguous for its mismatch of the knowns and unknowns, so

$$p * \mu^2 + q * \mu + r = 0 \tag{10}$$

This equation is found suitable for this problem and here p, q, r are the constants which are taken for calculation convenience only which don't have any practical significance. Since it was assumed of degree 2 and order 1 it needs at least 2 floor loads to obtain the solution. Which means the equation is solved initially for first 2 floor loads, after that 2nd and 3rd, after that 3rd and 4th, and so on so that the equation was validated for all the floor loads of the given benchmark building. This solvation will trigger 5% of error/ambiguity which could be neglected or ignores for its miniature measure.

3.6 Obtained Mode Shape

After a compressive evaluation and solvation of the equation of motion we arrive to an empirical value of the lateral deflection or displacement which gives the values for plotting the mode shape. This node was selected as since this mode is thought to be the most likely, it comprises almost 95% of the mass of the structure that is being analyzed.

It is not feasible to analyze all mode forms due to the non-triviality of the integral solution. Thus, the analytical process is streamlined by concentrating on the mode with

considerable mass engagement. The solution is tabulated in Table 1. The mode shape has been plotted for floor distance along y axis and the values of the empirical solution along x- axis the schematic representation is shown in Fig. 3.

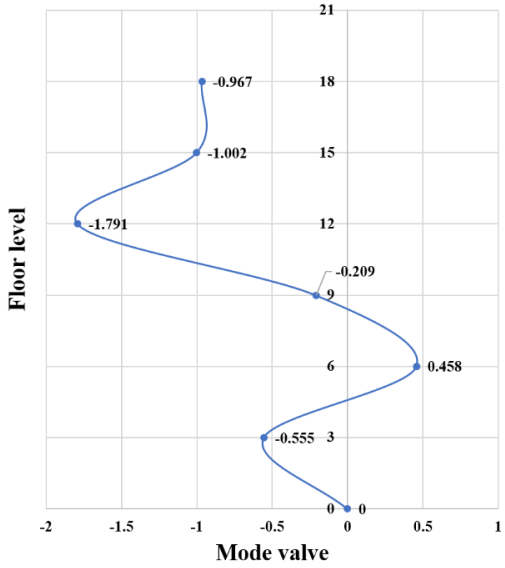

Fig. 3. Mode shape

Table 1. Solution for the displacement

Solution	
S1	S2
-0.555	0.458
-0.209	-1.791
-1.002	-0.967

3.7 Proposal for Positioning

When there are quantification constraints of the MR Damper, i.e. These are available at different capacity there might arrive a situation where the damper capacity may not arrive to meet the criteria for positioning in a structure. In such case this kind of positioning makes a crucial play and it also identified that the reduction of the displacement at substantial measures i.e. It was identified that this kind of positioning is 23% more efficient than the conventional practice of positioning. Since the final damping force was breakdown to availability of the dampers this kind of positioning found to be elemental. The following Fig. 4 represents the efficient positioning of dampers.

3.8 Constraints for Different Cases

Keeping in view the type of energy dissipation from the damper this kind of positioning was restricted for heavy heat dissipation. That is if the chances of heat dissipation were found at very heavy levels this is restricted by some other parameter like placing the different capacity dampers to ameliorate the worst possible effect of physical damage to the equipment. Despite the type of energy dissipation there is possibility of physical demolishment of the damper by itself, if the load acting on the damper exceeds its capacity, in such case a combination of dampers of different capacity must take with practical justification and ensure the avoidance of structure cracking. So, this kind of positioning

was restricted if there is unequal mitigation of energy dissipation between them, and some of the configuration flaws are also contribute for restricting this kind of positioning.

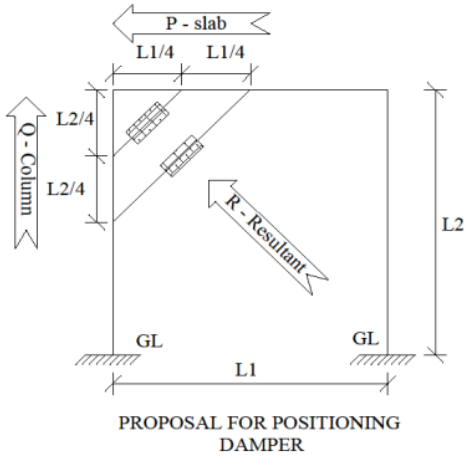

Fig. 4. Schematic representation of proposed positioning

3.9 Elements of Structure Involved

The proposed positioning involves the load acting due to the slab normal to the surface of the slab. It's not only the load due the self-weight of the beam and slab's but it includes the impulse force due to the earthquake loading (both lateral and normal to the plane of the structure) and the cumulative increase in the normal load due to variation in the beam and column size across the different locations of the structure. The contribution of the column i.e. the load acting due to the succeeding column along that joint and the upward or downward thrust due to the oscillations of the structure for different intensified earthquake loadings. Among these two the percentage share of the elements (beams & columns) mentioned changes depending on the direction of the earthquake loading, natural frequency, natural time and mode shape of the structure.

3.10 Load Contribution by the Elements (P & Q)

Let the load contributed by the slab and beams be assumed as 'P', the component P contains both static and dynamic load and combination of both as an external aggressive load (earthquake load). The static load includes the self-weight, dead load due to the existing things on that slab. The dynamic load includes the increasing the load with respect to time frame, it may be external or internal loading our case deals with the external loading i.e. earthquake loading which was assumed to have sine wave form. Due to this dynamic loading, there is chance of impulse force acting on the different slabs the ultimately damages the extreme columns of the structure depending on the oscillation of the structure. The 2nd elemental force that contributes to this kind of positioning was the thrust due to the column which is multi directional. The factors that are involved for producing the thrust include the natural frequency of the structure, time period, intensity of the external earthquake loading, column sizes at different storeys and symmetry of the structure. The thrust is produced due to lateral movement of the structure due to the external aggressive force impacting on the structure.

3.11 Resultant Force Vector and Its Validation

The force due to slab and beams will contribute to the P force acting is impulsive in nature when external aggressive force act on the structure, there will be no issue when there is no

external force acting on the structure. When there is coincidence of these two elemental forces the worst effect on the extreme columns were felt and observed as well. This could become the criteria for positioning to take the load due to its elemental force contribution. Since the direction and magnitudes of the two forces was identified to be measurable the vector notation was assumed to ease the calculations. So resultant vector was formed which is a virtual force vector that is obtained by calculating through vector algebra which can be given as 'R'.

$$R = \sqrt{P^2 + Q^2 + 2 * P * Q * cos\theta} \tag{11}$$

The resultant vector has nothing to contribute in practicality but it is used only for calculation purposes, if the external aggressive force acting on the structure in the direction of the resultant force the load can be spitted for P & Q by maintaining the proportionality for beams and columns.

3.12 Validation

This kind of positioning is not required at all the joints of the structure, its only required where the load acting at joint does not match with the capacity of the damper. So due to the mismatch of the load and capacity of the damper the load has been breakdown to the availability of the dampers, and they are placed keeping in mind the restrictions. This is also used where the worst point of affect was found, it was generally identified where the coincidence of the sine wave form and the exponential function occurs. As per the obtained mode shape the points are located depending on the empirical values achieved as a measure of the intensity of the force function. So, if the damper was placed/positioned, the loads taken by the pistons on both sides can be analyzed easily and the capacity of the damper required at that point is estimated as well

3.13 Exceptional Case and Practical Convenience

Since assumed earthquake have harmonic profile of motion there might be a case where the direction P & Q are in the opposite direction at the resultant can be obtained by taking the divergence of the force vector with respect to that point. Practical convenience: This not only reduces the displacements by substantial measure but also creates the spatial environment and aesthetic visual ambience when compared to the conventional practice of positioning.

4. Distribution of MR Dampers

4.1 Modal Mass and Its Significance for This Case

The mode shape which is obtained by this comprehensive mathematical modelling and its modal mass was evaluated by the formula.

$$[M]_k = \frac{[\sum(w_i * \varphi_{ik})]^2}{g * \sum(w_i * \varphi_{ik}{}^2)} \tag{13}$$

The mass for each slab was found out and compared with the normal mass by inclusion of the participation factor to it, which eventually results in an average of 96.42% mass involvement which conveys that our mode shape calculated was as per the objective mentioned. This modal mass is used as a criterion for distribution of the dampers along each floor and it also used as the criteria for load break down to allot the dampers of different damping capacity.

4.2 Development of a Simple Algorithm

The distribution of dampers across each joint is found uneconomical and through this algorithm no dampers are placed at the middle columns, only extreme columns are targeted through this algorithm. This algorithm finds its root from the concept of collisions (both elastic & inelastic). Assume a series of metallic balls when a single metallic ball is strike along the line of series of balls the force with which the 1st ball hits will be divides into number of balls taken into consideration. Immediately after hitting the 1st ball the energy will be conserved i.e. law of conservation of mass as well as law of conservation of energy was satisfied as of this case. So the as mentioned in the point 'c' the energy was transferred to the corresponding ball by the above laws by maintaining the proportionality with respect to the applied force on the initial ball. In this case of distribution of dampers, it was used to place all the dampers only along the extremely located columns at each and every floor on different constraints the last but one series of the extremity was used at certain cases only. Here the force is the external aggressive force i.e. earthquake loading, and the conservation of energy takes place between the columns with beams as median between them and the laws are sufficiently satisfied.

4.3 Participation Factor and Its Significance

For real systems there is often mass participating in the forcing function (such as the mass of ground in an earthquake) and mass participating in inertia effects (the mass of the structure itself, Meq). The modal participation factor is a comparison of these two masses. In this case the modal participation factor is given by p_k

$$p_k = \frac{[\sum w_i * \varphi_{ik}]^2}{\sum w_i * \varphi_{ik}{}^2} \tag{14}$$

In the above formula W with its suffix, I is generally taken as load due to each floor and'φ_ik' is the term stating the empirical solution of the mode shape.

4.4 Comprehensive Charting and Detailing

The technique was then used to transfer the load to the column endpoints after determining the modal mass for different slab loadings. The 90kN, 30kN, and 20kN-rated damper holes on each column at the extremities corresponded to the modal mass breakdown for the available capacities. Charts were used to record the distribution of loads among the various types of dampers according to their capabilities.

4.5 Project Developments

- Case 1: An optimization of 17.71% is obtained by using only 20kN and 30kN dampers. Base shear and seismic response estimates for the six-story benchmark structure are the parameters taken into consideration.
- Case 2: An optimization of 45.84% was obtained by doing a breakdown for three damper variants: 90kN, 30kN, and 20kN. Here, the six-story, three-bay benchmark building's modal mass and seismic response are among the variables that were taken into consideration.

- Case 3: By using 200kN dampers alone for analysis, efficiency was raised by almost 4%, yielding an optimization value of 49.66%. Similarly, a cost decrease of around 82.86% was calculated, contingent on damper costs.

4.6 Finalized Distribution

Following the determination of the load distribution breakdown to the structure's extreme columns, charts were created for each floor and joint in both the XZ and YZ directions. Because the benchmark building is symmetrical in both directions, it was sufficient to track one route and replicate the other. These charts, which are numbered 1 through 13, list the different types and quantities of dampers utilized each level. To make purchasing and actual use easier, the number of each damper variety was also tallied. Lastly, the percentage of cost reduction was mentioned, which was in line with the main goal of the project.

4.7 Detailing Along Each Floor Was Tabulated in XZ & YZ Directions

A thorough schematic showing the distribution and placement of dampers on each level, together with their precise locations, is given in Charts Nos. 1 through 10. The YZ direction needs the same amount of dampers as the XZ direction because of the structural symmetry that has been noticed. The positioning need, where each chart shows whether the suggested damper placement is customary (No. 1) or essential (No. 2) at different places inside the structure, depends on this alignment.

5. Result and Discussion

Table 2 shows the details of the G+6 Benchmark building. Fundamental natural time period (Ta), zone factor (Z), importance factor (I), response reduction factor (R), Sa/g, horizontal seismic coefficient (Ah) is obtained from IS 1893 part 1 2016. Calculation of Base Shear and Load Distribution along each floor is shown in Table 3. The Table 3 gives details regarding each storey's net load, height, and seismic weight inside the structure. The seismic weight multiplied by the height is computed. The base shear and load distribution of the structure may be ascertained using the seismic weight and height of each story.

Table 2. Details of the G+6 Benchmark building

Height Of Structure (h)	18
Base Dimension (d)	5
Fundamental Natural Time Period (Ta)	0.724
Zone Factor (Z)	0.16
Importance Factor (I)	1.5
Response Reduction Factor (R)	3
Sa/g	1.879
Horizontal Seismic Coefficient (Ah)	0.075
Total Seismic Weight 'W'(KN)	31218
Design Base Shear (Vb)	2341.35
Height Of Gf In (m)	3
Sum (W*H)	190419.75

The mode comprising more than 95% of the mass may be found by analyzing the mode forms of the structure using the net load of each storey. Determining the worst point of effect of the load impulse and improving damper location depend heavily on the mode shape involving more than 95% of the mass. Fig.5 shows an illustration of the load distribution laterally over a structure is provided by a lateral load distribution curve. The force or pressure applied to the structure in a horizontal direction, as during an earthquake, is referred to in this context as the lateral load.

The distribution of the load at the building's various levels or floors is shown by the curve. It aids in comprehending the variance in load distribution and may be applied to ascertain

the best location and arrangement of dampers to regulate the building's seismic reaction. Researchers can install dampers where greater control is needed and reduce the number of dampers in regions with lesser load distribution by evaluating the curve to determine which floors or levels have concentrated and distributed loads.

Through an evaluation of the efficiency score derived from the optimization process, the curve can also shed light on the efficacy of the chosen damper configuration. The shear distribution details, and stiffness calculation is shown in Fig. 6 and Table 4. The distribution of forces acting perpendicular to the floor planes is known as the shear distribution. Understanding the building's response to seismic forces and how those forces are dispersed throughout the structure requires knowledge of this information. The best location and arrangement of magnetic resonance dampers (MR dampers), which are control devices used to lessen vibration and absorb energy during an earthquake, may be determined with the aid of the shear distribution. Researchers can determine which floors or parts of the structure encounter higher shear forces and may need more dampers for successful control by examining the shear distribution. Together with further computations and studies, the shear distribution information shown in Fig. 6 may be utilized to establish the best location and quantity of dampers for regulating the building's seismic reaction. In Table 4 varying columns have varying stiffness values; higher values indicate more resistance to deformation. The width and depth of the columns have an impact on how rigid they are as well. The total stiffness of the interior and exterior columns is considered in the net stiffness. All things considered, the chart offers details regarding the stiffness and sizes of various columns, which may be helpful in comprehending the building's structural characteristics. The seismic weight of building is calculated by adding full amount of dead load and imposed load of 25% as per IS 1893 (part 1): 2016. While computing the seismic weight of each floor, the weight of columns and walls in any storey shall be equally distributed to the floors above and below the storey. The net load on each floor is calculated by the difference between lateral shear force (Q) and the loads on the prior floor. The lateral shear force (Q) at each floor is calculated by an equation as per IS 1893 (part 1): 2016

$$Q_i = v_B \frac{w_i h_i^2}{\sum w_j h_j^2} \tag{15}$$

Table 3. Design calculation excel for G+6 Benchmark building

Seismic Weight (W) In kN		Height Of Storeys (H) In m		W*H (kNm)	Q (Kn)	Net Load (kN)
GF	7348.5	GF	0	0	0	2341.352
F1	6972	H1	3	20916	257.178	2341.352
F2	5751.75	H2	6	34510.5	424.332	2084.174
F3	4247.25	H3	9	38225.25	470.008	1659.842
F4	3417.75	H4	12	41013	504.285	1189.834
F5	2299.5	H5	15	34492.5	424.111	685.549
R	1181.25	H6	18	21262.5	261.438	261.438

Table 4. Stiffness calculations

Floors	Ext Column Dimension		Int Column Dimension		Moment Of Inertia		Stiffness		
	Breadth (m)	Depth (m)	Breadth (m)	Depth (m)	Ext I (N/m)	Int I (N/m)	Ext K (N/m)	Int K (N/m)	Net K (N/m)
F1	0.6	0.6	0.65	0.65	0.011	0.015	122.223	166.667	2311.112
F2	0.6	0.6	0.65	0.65	0.011	0.015	15.27778	20.8334	288.8895
F3	0.55	0.55	0.6	0.6	0.008	0.011	3.29219	4.5268	62.552
F4	0.55	0.55	0.6	0.6	0.008	0.011	1.38889	1.9098	26.3896
F5	0.5	0.5	0.55	0.55	0.006	0.008	0.53334	0.7112	9.9564
R	0.5	0.5	0.55	0.55	0.006	0.008	0.30865	0.4116	5.762

Table 5. Characteristics

Young's modulus	25000
Total number of external columns	8
Total number of internal columns	8
Characteristic compressive strength	25

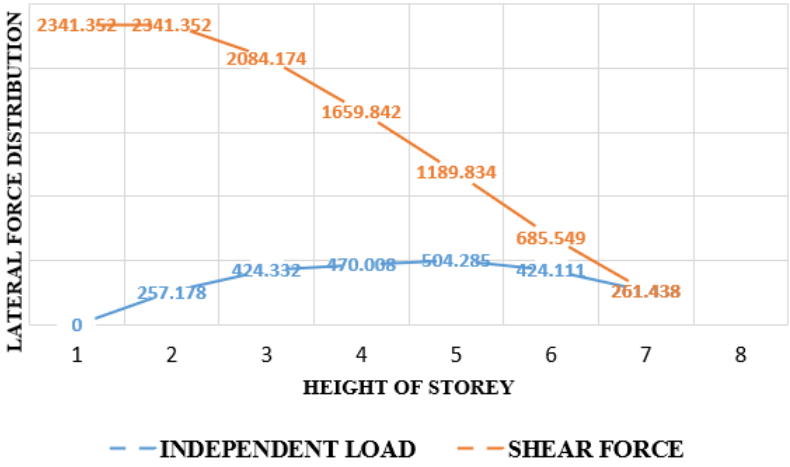

Fig 5. Lateral load distribution curve

General equation of motion:

$$m * xm * \ddot{x} + c * \dot{x} + k * x = e^{-t} * \tag{16}$$

Formula Used:

$$K = \frac{12*E*I}{l^3} \quad k_{NET} = \sum_{i=1}^{16} K_i \tag{17}$$

Complementary function:

$$r_{1,2} = \frac{-c}{m} \pm \sqrt{\frac{c^2}{4 \times m^2} - \frac{k}{m}} \tag{18}$$

$$x = p \times e^{r_1 t} + q \times e^{r_2 t} \tag{19}$$

Integral:

$$\frac{e^{-t} \times \sin(\omega t)}{m \times D^2 + k} \tag{20}$$

Modified complimentary function

Solution for this case of problem

$$x = A \times \sin(\omega t) + B \times \cos(\omega t) \tag{21}$$

5.1 Result of Case 1: When 20kN,30kN Load Damper Is Used

Table 6 lists how many dampers are needed at each floor for the specified loads of 20 and 30 kN. There are eight dampers needed for each of the first, second, and ground floors. Each of the third and fourth levels needs four dampers. Two dampers are needed for the fifth story. Based on Table 7 a 20 kN load is applied to a total of 14 dampers.

Table 6. The required quantity of dampers for each floor

Required Number of Dampers	
GROUND FLOOR	8
FLOOR 1	8
FLOOR 2	8
FLOOR 3	4
FLOOR 4	4
FLOOR 5	2
TOTAL	34

A load of 30kN is applied to a total of 20 dampers. Using a total of 14 dampers allows for the best possible damper location and distribution for the specified load of 20 kN and 30 kN. This distribution lessens structural damage during an earthquake and helps regulate the building's seismic reaction. The distribution places the greatest number of dampers on the ground level, first floor, and second floor, and the lowest number on the fifth story.

Table 7. Total number of 20 & 30kN dampers

Distribution Of Dampers at Different Floors		
FLOORS	20 kN	30 kN
GF	0	8
F1	0	8
F2	4	4
F3	0	4
F4	4	0
F5	2	0
TOTAL	10	24

5.2 Result of Case 2: When 20 kN,30 kN & 90 kN Load Damper Is Used

The load capacity affects how dampers are distributed. The number of dampers needed for the first, second, and ground floors is the same for all load capacities. Compared to the other levels, the third floor needs less dampers to support the 30kN load. For all load capacities, the same number of dampers are needed on the fourth and fifth floors. Regardless of the load capacity, the building has a total of 44 dampers.

Table 8. The required quantity of dampers for each floor

Required Number of Dampers	
GROUND FLOOR	8
FLOOR 1	8
FLOOR 2	8
FLOOR 3	4
FLOOR 4	8
FLOOR 5	8
TOTAL	44

Table 9. Total quantity of 20 kN, 30 kN & 90 kN dampers @ different floors

Distribution of Dampers at Different Floors			
	90 kN	20 kN	30 kN
GF	8	0	0
F1	8	0	0
F2	4	4	0
F3	4	0	0
F4	0	0	8
F5	0	8	0
TOTAL	24	12	8

5.3 Result of Case 3: When Using A 200kN Load Damper

The number of dampers required at each floor for the 200 kN prescribed loads is listed in Table 10. Eight dampers are required for the ground levels, four dampers are required for the first floor, and no dampers are required for the second story. Two dampers are required for each of the third and fourth tiers. It takes one damper to cover the fifth storey. There are a total of 17, 200 kN dampers dispersed over many floors.

Table 10. Required number of dampers at different floors

Required Number of Dampers	
GROUND FLOOR	8
FLOOR 1	4
FLOOR 2	0
FLOOR 3	2
FLOOR 4	2
FLOOR 5	1
TOTAL	17

5.4 Non-linear Time History Analysis

The most accurate method for representing the behavior of a structure under seismic stresses is thought to be nonlinear time history analysis. In order to account for the nonlinear properties of the support system, this technique entails methodically integrating the equations of motion of the system. It calculates the displacements, peak accelerations, and forces of the system for each time step and determines their maximum values during seismic occurrences. To accomplish accurate earthquake effect simulations, SAP2000 V19 software was used to perform nonlinear time history analysis on the building models. Three grid lines each in the x and z directions and six grid lines in the y direction make up the grid system used in SAP2000's structural design. These grid lines are spaced five meters apart in the x and z directions and three meters apart in the y direction. The

material parameters are defined in accordance with Indian norms; 25 kN/m^3 of density, 20,000 MPa of modulus of elasticity (E), 0.2 Poisson's ratio, 1E-05 (1/°C) coefficient of thermal expansion (α), and 25 MPa of compressive strength were chosen for the concrete. For reinforcing bars, the minimum yield strength (Fy) is 420 MPa, the minimum tensile strength (Fu) is 550 MPa, the predicted yield stress (Fyc) is 420 MPa, and the Young's modulus (E) is 200,000 MPa. The coefficient of thermal expansion (α) is 1.2E-05 (1/°C). 16d longitudinal bar sizes and 8d confinement bar sizes are used to define columns and beams. In accordance, section attributes are assigned, and 0.18 meters is the membrane and bending thickness. Diaphragm limitations are applied and joint constraints are fixed. Using El Centro earthquake data for the load case type and scaling by 9.81E-3, a time history function is created. Dead loads are defined as mass sources, and the output time step size is fixed at 0.005 seconds. Two-way distribution of uniform area loads of 10 kN/m^2 is applied to the frames. Frames are allocated element loads, and load cases are prepared for evaluation. The inter-story drift during the El Centro earthquake was found to exceed the allowable limit in all structures, according to the study results. The permissible maximum for inter-story drift is 0.004 times the storey height, under IS 1893 part 1 (2002). The maximum permissible inter-story drift value for a structure with a storey height of eighteen meters is determined by this:

$$\Delta = 0.004 \times h = 0.004 \times 3 = 0.012m \tag{22}$$

The results of the investigation show that during the El Centro earthquake, the inter-story drift in every building surpassed the allowable limit. The maximum permitted inter-story drift, under IS 1893 part 1 (2002), is 0.004 times the height of each storey. This rule establishes the maximum amount of inter-story drift for a structure with eighteen-meter-tall storeys.

6. Conclusion

By using this mathematical modeling, the complementary function and particular integral's complexity were addressed, leading to a solution with over 90% confidence. Accuracy and project scope may be varied for higher storeys, improving damper distribution efficiency, by varying the degree and order of the characteristic equation. By reducing displacements substantially (23% more effectively than standard approaches), the suggested positioning strategy improved space usage and attractiveness. Moreover, this decreased deflection, especially for P and Q intensities, demonstrating the efficacy of the dampers. As to IS 1893 (part 1) 2002, the maximum allowable inter-storey drift is 0.012 meters, or 0.004 times the storey height. To make sure drift stayed within this bound, dampers were positioned strategically. The worst-case impact analysis (mode shape and force function correlation) was used to determine the ideal damper placements and amounts. To handle the stress on extreme columns, only 20kN (14#) and 30kN (20#) dampers were utilized, depending on availability. To limit seismic response, the study proposes a methodical approach for determining the best location and distribution of magnetorheological (MR) dampers in a benchmark 6-story structure. To identify the worst location for damper positioning, the authors provide a mathematical modelling technique that makes use of the maximal force function and mode shape. This method aids in lowering the price of damper allocation in construction projects. The optimum damper distribution for several load scenarios, including 20kN, 30kN, 90kN, and 200kN, is provided in this study. There are 17 dampers utilized overall for a 200kN load, with the distribution differing throughout floors. An efficiency score of 49.616 from the optimization process illustrates how effective the chosen damper configuration is. The practicality of the suggested damper placement—which, in contrast to traditional methods, not only minimizes displacements but also produces an aesthetically pleasing

spatial environment—is also covered in the study. The precise standards or selection process for the benchmark building, as well as the seismic reaction factors taken into consideration for optimization, are not covered in this work. The financial ramifications of the damper placement and distribution are not thoroughly examined in the article. The cost reduction based on the optimization outcomes is only mentioned in general terms. The suggested damper location may not work in real-world situations due to practical restrictions, installation requirements, or possible conflicts with other building systems. These issues are not covered in the article. Future research in seismic response control may find great use for the methodical approach to damper installation and distribution that is presented in this study. Future studies can build on and enhance the mathematical modelling technique employed in this study, which involves mode shape and maximal force function, to increase the precision and effectiveness of damper optimization. Future research on comparable benchmark buildings or structures might utilize the optimal damper distribution results from this study as a guide since they offer information on the quantity and positioning of dampers needed for efficient seismic response management.

References

[1] Stein RS. The role of stress transfer in earthquake occurrence. Nature. 1999;402(6762):605-609. https://doi.org/10.1038/45144

[2] De Silva CW. An algorithm for the optimal design of passive vibration controllers for flexible systems. J Sound Vib. 1981;75(4):495-502. https://doi.org/10.1016/0022-460X(81)90437-5

[3] Ibidapo-Obe O. Optimal actuators placements for the active control of flexible structures. J Math Anal Appl. 1985;105(1):12-25. https://doi.org/10.1016/0022-247X(85)90094-0

[4] Zhang RH, Soong TT. Seismic design of viscoelastic dampers for structural applications. J Struct Eng. 1992;118(5):1375-1392. https://doi.org/10.1061/(ASCE)0733-9445(1992)118:5(1375)

[5] Milman MH, Chu CC. Optimization methods for passive damper placement and tuning. J Guid Control Dyn. 1994;17(4):848-856. https://doi.org/10.2514/3.21275

[6] Peng Y, Zhang Z. Optimal MR Damper-Based Semiactive Control Scheme for Strengthening Seismic Capacity and Structural Reliability. J Eng Mech. 2020;146(6). https://doi.org/10.1061/(ASCE)EM.1943-7889.0001768

[7] Elias S, Matsagar V. Seismic response control of steel benchmark building with a tuned mass damper. Asian J Civ Eng. 2020;21(2):267-280. https://doi.org/10.1007/s42107-019-00206-1

[8] Takewaki I, Uetani K. Optimal damper placement for building structures including surface ground amplification. Soil Dyn Earthq Eng. 1999;18(5):363-371. https://doi.org/10.1016/S0267-7261(99)00007-X

[9] Shukla AK, Datta TK. Optimal use of viscoelastic dampers in building frames for seismic force. J Struct Eng. 1999;125(4):401-409. https://doi.org/10.1061/(ASCE)0733-9445(1999)125:4(401)

[10] Singh MP, Moreschi LM. Optimal placement of dampers for passive response control. Earthq Eng Struct Dyn. 2002;31(4):955-976. https://doi.org/10.1002/eqe.132

[11] Lopez Garcia D, Soong TT. Efficiency of a simple approach to damper allocation in MDOF structures. J Struct Control. 2002;9(1):19-30. https://doi.org/10.1002/stc.3

[12] Villarreal K, Wilson C, Abdullah M. Effects of MR damper placement on structure vibration parameters. In: Proceedings of the 2004 Earthquake Engineering Symposium for Young Researchers. 2004 July. 279;5-8.

[13] Bharti SD, Dumne SM, Shrimali MK. Seismic response analysis of adjacent buildings connected with MR dampers. Eng Struct. 2010;32(8):2122-2133. https://doi.org/10.1016/j.engstruct.2010.03.015

[14] Cha YJ, Agrawal AK, Phillips BM, Spencer Jr BF. Direct performance-based design with 200 kN MR dampers using multi-objective cost effective optimization for steel MRFs. Eng Struct. 2014;71:60-72. https://doi.org/10.1016/j.engstruct.2014.04.023
[15] Uz ME, Hadi MN. Optimal design of semi-active control for adjacent buildings connected by MR damper based on integrated fuzzy logic and multi-objective genetic algorithm. Eng Struct. 2014;69:135-148. https://doi.org/10.1016/j.engstruct.2014.03.006
[16] Cetin S, Zergeroglu E, Sivrioglu S, Yuksek I. A new semiactive nonlinear adaptive controller for structures using MR damper: design and experimental validation. Nonlinear Dyn. 2011;66(4):731-743. https://doi.org/10.1007/s11071-011-9946-0
[17] Wang H, Li A, Jiao C, Spencer BF. Damper placement for seismic control of super-long-span suspension bridges based on the first-order optimization method. Sci China Technol Sci. 2010;53(7):2008-2014. https://doi.org/10.1007/s11431-010-4009-1
[18] Kori JG, Jangid RS. Semi-active MR dampers for seismic control of structures. Bull N Z Soc Earthq Eng. 2009;42(3):157-166. https://doi.org/10.5459/bnzsee.42.3.157-166
[19] Cha YJ, Agrawal AK, Friedman A, Phillips B, Ahn R, Dong B, Dyke SJ, Spencer BF, Ricles J, Christenson R. Performance validations of semiactive controllers on large-scale moment-resisting frame equipped with 200-kN MR damper using real-time hybrid simulations. J Struct Eng. 2014;140(10). https://doi.org/10.1061/(ASCE)ST.1943-541X.0000982
[20] Aydin E. Optimal damper placement based on base moment in steel building frames. J Constr Steel Res. 2012;79:216-225. https://doi.org/10.1016/j.jcsr.2012.07.011
[21] Soto MG, Adeli H. Placement of Control Devices for Passive, Semi-Active, and Active Vibration Control of Structures. Scientia Iranica. 2013;20(6):1567-1578.
[22] Truong DQ, Ahn KK. MR fluid damper and its application to force sensorless damping control system. In: Smart Actuation and Sensing Systems-Recent Advances and Future Challenges. 2012;83-425.
[23] Cruze D, Hemalatha G, Jebadurai SVS, Sarala L, Tensing D, Christy SJE. A review on the magnetorheological fluid, damper and its applications for seismic mitigation. Civil Eng J. 2018;4(12):3058-3074. https://doi.org/10.28991/cej-03091220
[24] Daniel C, Hemalatha G, Sarala L, Tensing D, Sundar Manoharan S. Magnetorheological Fluid with Nano Fe3O4 for Performance Enhancement of MR Damper for Seismic Resistance of Steel Structures. In: Key Eng Mater. 2018;763:975-982. https://doi.org/10.4028/www.scientific.net/KEM.763.975
[25] IS 1893 : 1962. Recommendations for earthquake resistant design of structures.